

## Safety factor calibration for bridge concrete girders

Rita C. Silva<sup>\*1</sup> and Christian Cremona<sup>2a</sup>

<sup>1</sup>Faculty UnB Gama, Complexo de Educação, University of Brasília, Cultura, Esporte e Lazer,  
72405-610, Gama, Brazil

<sup>2</sup>Directorate for Research and Innovation, Ministry of Ecology, Energy, Sustainable Development and Sea,  
Tour Pascal, 92055 La Défense, France

(Received April 22, 2012, Revised November 15, 2013, Accepted December 9, 2013)

**Abstract.** Safety factors proposed in codes CEB, B.A.E.L 91 and EUROCODE 1 cover a great number of uncertainties; making them inadequate for the assessment of existing structures. Suitable safety factors are established using a probabilistic assessment, once real dimensions, materials strength and existing structures deterioration mechanisms are taken into account. This paper presents a calibration method for safety factors using a typical set of RC bridges in France. It considers the principal stages of corrosion provoked by CO<sub>2</sub> and Cl<sup>-</sup> penetration and threshold indexes ( $\beta_0$ ) for existing structures. Reliability indexes are determined by the FORM method in the calibration method.

**Keywords:** calibration; corrosion; reinforced concrete; reliability; safety factors

---

### 1. Introduction

Bridges play an important role in human life as their construction can boost the social and economic development of a region. However, over time, these structures seem to degenerate and suffer a loss in performance.

The main causes of degradation are the increase in load (mainly due to the traffic) and material degradation (caused by exposure to aggressive agents). This degradation can be aggravated in many locations by ineffective maintenance programs. This may lead to the loss of life as mentioned by Petryna and Kratzig (2005), Cui *et al.* (2011).

In the last thirty years, many studies (Necati *et al.* 2008, Xiangyang and Pei 2010, Cui *et al.* 2011), have focused on the life cycle prediction of bridges and deterioration mechanisms. This is relevant since many existing bridges are old and have had their bearing capacity affected over the years.

Reinforced concrete (RC) bridges use one of the most common materials in civil engineering. However, until today, not much is known about the influence of environmental conditions on reinforced concrete's mechanical and physical behavior, and also on its performance as a construction material. As a result any evaluation of RC structures durability will be a very difficult task. In addition, even when high quality materials are utilized in the structure's construction, a

---

\*Corresponding author, Professor, E-mail: [ritasilva@unb.br](mailto:ritasilva@unb.br)

<sup>a</sup>Ph.D., E-mail: [cremona@lcpc.fr](mailto:cremona@lcpc.fr)

long service life for the structure cannot be assured.

Moreover, a long service lifetime depends on the history of loads applied to the structure and on the structure's constituent materials. Nevertheless, the major degradation mechanisms acting on the RC structures is the corrosion of reinforcement steel and, studies in this field still be very relevant Sharifi and Paik (2010), Czarnecki and Nowak (2008).

The integrity of RC structures is associated with the penetration of polluting agents. In France, the assessment of a typical set of RC bridges showed that carbon dioxide (found in the atmosphere) and chloride ions (from de-icing salts) are usually such agents. So, in the absence of any aggressive agent, reinforcement is expected to be passivated. Actually, physical conditions of the concrete can be modified if any polluting agent is present, exposing the reinforcement to harmful conditions.

First aggressive agents penetrate through the pores of the concrete cover. Then the amount of  $\text{CO}_2$  and  $\text{Cl}^-$  increases near the steel bars and the basic environment that usually surrounds the reinforcement is modified by these agents. In the case of chloride ions its concentration can reach a critical value, called critical chloride content (threshold chloride content), in which steel is no longer passivated. In the carbonation case, the parameter to be considered is the concrete pH, which critical value is  $\text{pH} \leq 9$ . Exceeding threshold values can cause loss of durability in structural members and premature deterioration process (initiation time of corrosion).

Life-cycle performance of deteriorating structures comprises two main cycles. The first one corresponds to the loss of durability due to penetration of aggressive agents through the concrete cover pores, but reinforcement is not yet corroded. The second cycle starts at a certain time  $T_i$ , when steel corrosion is initiated, and it finishes when the serviceability conditions are no longer fulfilled.

The second cycle can be divided into three sub-cycles named:  $T_{crack}$  (concrete cover cracks due to rust expansion in time);  $T_{ser}$  (the amount of rust formed by the metal loss is sufficient to generate visible cracks). The width of concrete cracks increases up to an allowable crack size (0.3mm according to many codes –serviceability limit state). Finally, at time  $T_{spal}$  crack width is very large (1.0 mm admissible) so that spalling occurs. The third sub-cycle finishes when the performance index ( $\beta$ ) has reached an allowable threshold value  $\beta_0$  given by standards or regulations for existing structures, when available. This performance time is denoted  $T_{\beta_0}$ . Of course, this does not mean that the structure is unsafe or has failed, but it indicates that the structure no longer fulfills the ultimate requirements as prescribed by standards.

Ultimate requirement is expressed in terms of the probability of failure at the ultimate limit state (flexural limit state) in a probabilistic format. This probability of failure is indeed a notational probability of failure and should not be confused with any failure statistics.

Before reaching the allowable level ( $T_{\beta_0}$ ), it may be interesting to determine some specific instants related to corrosion damage levels. Here, the time  $T_{10\%}$ , when 10 % of the bottom reinforcement layer is lost to corrosion, will be considered.

In this paper, an approach to predicting life-cycle performance is proposed for RC girders exposed to chloride and carbonation attacks. The proposed methodology has been applied to a set of RC bridges in France subjected to a range of environmental conditions. A probabilistic assessment is considered to analyze the degradation profile and loss of performance due to the combination of several factors, previously available in scattered data. This analysis has two interesting features. The first one presented in Silva (2004), Silva and Cremona (2004), provides the prediction tables for maintenance engineers, which are easy to use. The second which will be analyzed in this paper, gives the partial safety factors applied to resistance and loading variables. It

considers the most important cycles of corrosion phenomena and the minimal acceptable performance level  $\beta_0$ . Therefore, safety factors which are more appropriate to the study of loss in the main reinforcement area (loss of resistance strength) are obtained probabilistically.

## 2. Life-cycle performance prediction

Classical models are used in this paper for describing the various cycles of the corrosion process. Carbonation or chloride ingress can be expressed in terms of diffusion laws. Concrete cracking is obtained by using elastic properties in connection with the rust expansion and the tensile strength in the concrete. The loss of reinforcement area is calculated by using the steel corrosion rate.

### 2.1 Modeling chloride-induced corrosion initiation

Admitting that the constant chloride diffusion coefficient  $D_0$  (Brime 2001, Vu Kin and Stewart 2000, Thoft-Chirstensen 2000) is introduced, a special case of the well-known Fick's general diffusion law is obtained

$$\frac{\partial C}{\partial t} = D_0 \frac{\partial^2 C}{\partial x^2} \quad (1)$$

where  $D_0$  is the chloride diffusion coefficient (in  $\text{cm}^2/\text{s}$ ). If the initial concentration in the sample is equal to zero, then the solution of differential Eq. (1) is

$$C(x,t) = C_s \left( 1 - \text{erf} \left( \frac{x}{\sqrt{4D_0 t}} \right) \right) \quad (2)$$

where  $C(x,t)$  is the chloride content (as a percentage of the cement weight) for depth  $x$  at time  $t$ .  $C_s$  is the surface content (as a percentage of the cement weight).  $\text{erf}$  is the error function. If  $x = cp$  and  $C(cp,t) = C_{cr}$ , where  $cp$  is the concrete cover and  $C_{cr}$  the critical chloride content, the corrosion initiation time can be expressed as

$$T_i = \frac{cp^2}{4D_0} \left( \text{erf}^{-1} \left( \frac{C_{cr} - C_s}{C_s} \right) \right)^{-2} \quad (3)$$

### 2.2 Modeling carbonation-induced corrosion initiation

The following empirical formula is generally used for carbonation prediction

$$x = K \sqrt{t} \quad (4)$$

where  $x$  is the carbonation depth;  $K$ , the carbonation constant ( $\text{m}/\text{t}^{0.5}$ ) and  $t$ , the exposure time. A guess value of  $K$  can be estimated from the following expression proposed by Papadakis (1991a)

$$K = \sqrt{\frac{2D_{\text{CO}_2} [\text{CO}_2]}{[\text{Ca}(\text{OH})_2] + 3[\text{C-S-H}] + 3[\text{C}_3\text{S}] + 2[\text{C}_2\text{S}]} \quad (5)$$

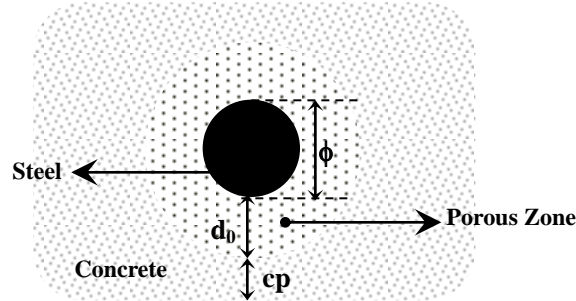


Fig. 1 Concrete cracking model using a thick-wall cylinder

where  $D_{CO_2}$  is the effective diffusivity of  $CO_2$  in carbonated concrete ( $m^2/s$ ) determined by the following empirical equation

$$D_{CO_2} = 1.64 \cdot 10^{-6} \varepsilon_p^{1.8} (1 - 0.01 HR)^{2.2} \quad (6)$$

where  $[CO_2]$  molar concentration of  $CO_2$  (gaseous phase) is in contact with concrete (mols per unit of volume);  $[Ca(OH)_2]$ ,  $3[C-S-H]$ ,  $3[C_3S]$  and  $2[C_2S]$  are the molar concentrations of cement components that participate in carbonation reactions in the concrete. Thus, the sum shown in Eq. (5) characterizes the total molar concentration of all carbonatable constituents expressed in  $CaO$ . The hardened cement paste porosity is  $\varepsilon_p$  and  $HR$  is the relative humidity, Papadakis *et al.* (1991b), Ishida and Maekawa (2000), Papadakis *et al.* (1991a). The corrosion initiation time of carbonation is given by

$$T_i = \left( \frac{cp}{K} \right)^2 \quad (7)$$

### 2.3 Modeling concrete cracking

The porous zone around the steel/concrete surface is progressively filled by corrosion products, which are less dense than the original reinforcement. When it is totally filled, the corrosion products create an expansive pressure at the interface between reinforcement and concrete. The pressure then induces concrete cracking.

The critical amount of corrosion products consists of two parts:  $W_p$ , the amount of corrosion products required to fill the porous zone and  $W_s$  the amount of corrosion products that generates cracking.  $W_p$  can be estimated by Liu and Weyers (1998)

$$W_p = \pi \rho_{rust} d_0 \phi \quad (8)$$

where  $\rho_{rust}$  is the density of corrosion products,  $d_0$  the thickness of the porous zone and  $\phi$  the original diameter of the steel bar.  $W_s$  can be estimated from the following equation Liu and Weyers (1998)

$$W_s = \rho_{rust} \left( \pi (\phi + 2 d_0) d_s + \frac{W_{st}}{\rho_{st}} \right) \quad (9)$$

where  $\rho_{st}$  is the steel density;  $d_s$  is the thickness of corrosion products needed to generate tensile stress and  $W_{st}$  is the mass of corroding steel. Based on the previous equations, the critical amount of corrosion products is given by

$$W_{crit} = \rho_{rust} \left( \pi(d_s + d_0)\phi + \frac{W_{st}}{\rho_{st}} \right) \quad (10)$$

If the reinforced concrete is modelled as a thick-wall cylinder subject to an internal radial pressure, as shown in Fig. 1, the thickness of corrosion products needed to induce tensile stress is

$$d_s = \frac{cp f_t}{E} \left( \frac{a^2 + b^2}{b^2 - a^2} + \nu_c \right) \quad (11)$$

where  $a = (\phi + 2d_0/2)$  and  $b = cp + (\phi + 2d_0/2)$ .

Eq. (11) is deduced from the equality between the pressure at the concrete-rust products interface and the minimum stress required to cause cracking of the concrete cover which is equal to the tensile strength of concrete.  $E$  is the concrete Young modulus,  $f_t$  the tensile strength of the concrete and  $\nu_c$  the concrete Poisson coefficient. The amount of corroding steel  $W_{st}$  is in general expressed as a proportion of  $W_{crit}$ :  $W_{st} = \alpha W_{crit}$ , Liu and Weyers (1998). The term  $\alpha$  depends on the types of corrosion products and for simplicity,  $\alpha$  is assumed to be equal to 0.57. Thus, Eq. (11) becomes

$$W_{crit} = \frac{\rho_{rust} \rho_{st}}{\rho_{st} - 0.57\rho_{rust}} \left( \pi \phi \left( \frac{cp f_t}{E} \left( \frac{a^2 + b^2}{b^2 - a^2} + \nu_c \right) + d_0 \right) \right) \quad (12)$$

The amount of corrosion products (kg/m)  $W_{rust}$  is supposed to be the solution of the following differential equation

$$\frac{dW_{rust}}{dt} = \frac{k_{rust}}{W_{rust}} \quad (13)$$

where  $k_{rust}$  is the rate of the rust production which is proportional to the corrosion rate  $i_{corr}$  ( $\mu\text{A}/\text{cm}^2$ ) and to the diameter  $\phi$  of reinforcement Liu and Weyers (1998)

$$k_{rust} = 0.383 \cdot 10^{-3} \phi i_{corr} \quad (14)$$

Integrating Eq. (14), the growth of rust products can be deduced as

$$W_{rust}(t) = \sqrt{2 \int_{T_i}^t k_{rust} dt} = \sqrt{2 k_{rust} (t - T_i)} \quad (15)$$

The amount of rust products at any time can be estimated and compared with Eq. (12) to define the time corresponding to cracking

$$\Delta t_{crack} = \frac{W_{crit}^2}{2 k_{rust}} \quad (16)$$

$$T_{crack} = T_i + \Delta t_{crack} \quad (17)$$

## 2.4 Modeling concrete crack width during corrosion

Concrete crack width is a very influential parameter on reinforcement corrosion Vu Kin and Stewart (2000). In this paper, the time necessary to reach two important crack widths is considered. The first one is the time needed to reach a crack width  $w_{serv}$ , equal to the allowable crack width required by standards, in this paper the value of 0.3mm is used and corresponds to the CEB allowable value, EUROCODE 1, BS 8110 standards. Cracking may also induce concrete spalling and in this case, a larger width  $w_{spal}$  is introduced. The value of 1.0mm is introduced in this paper for characterising this effect. Several authors Vu Kin and Stewart (2000), Andrade *et al.* (1993) propose

$$\Delta w = \gamma \Delta \phi \quad (18)$$

where  $\Delta w$  is the crack increment and  $\Delta \phi$  the loss of rebar diameter during  $\Delta t$ . The factor  $\gamma$  may be estimated by

$$\gamma = \frac{(\varphi - 1) \pi \phi}{\left( \frac{\phi/2}{\phi/2 + cp} + 1 \right) cp} \quad (19)$$

where,  $\varphi = \rho_{st} / \rho_{rust}$  is the ratio between steel density and corrosion product density, with values ranging from 2 to 4, Vu Kim and Stewart (2000). Thus, if  $\Delta w = w(t) - w_0$  and  $w(t) = w_0 + \gamma(0.0230 i_{corr})t$ , where  $w_0$  is the initial crack width (equal to 0) and  $w(t) = w_{serv}$ , assuming uniform corrosion, the time interval for reaching the crack width  $w_{serv}$  is

$$\Delta t_{serv} = \frac{w_{serv}}{\gamma (0.0230 i_{corr})} \quad (20)$$

and

$$T_{serv} = T_{crack} + \Delta t_{serv} \quad (21)$$

Similarly, the time interval to reach a crack width of 1.0mm is deduced assuming that  $\Delta w = w_{lim} - w_{serv}$ , where  $\Delta w = w(t) - w_0 \rightarrow w(t) = w_{spal} = 1.0\text{mm}$ ;  $w_0 = w_{serv}$ . Using the same reasoning to predict the spalling time, it becomes

$$\Delta t_{spal} = \frac{w_{spal} - w_{serv}}{\gamma (0.0230 i_{corr})} \quad (22)$$

and

$$T_{spal} = T_{serv} + \Delta t_{spal} \quad (23)$$

## 2.5 Cycles corresponding to large losses of reinforcement area

The final cycles of the RC's girders service life,  $T_{10\%}$  and  $T_{\beta_0}$ , are obtained respectively for a 10% deterioration in the initial reinforcement area of the bottom layer and for the minimal acceptable performance level  $\beta_0$  as defined by the standards. The determination of this target reliability is broadly described in the next section.

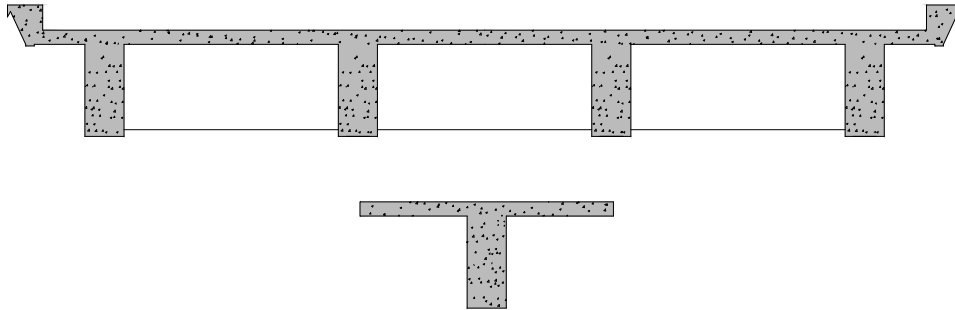


Fig. 2 Typical bridge cross section

Table 1 Characteristics of the RC bridges

Superstructure		Geometry			Cross section		
Girders	Cross-beams	Lanes	Width (m)	Length (m)	Height (m)	Web width (m)	Flange width (m)
4; 5; 6	5; 8	2; 3	10; 13	10 ;20; 30	0.75; 1.25	0.30; 0.50	2.00; 2.30; 2.50; 3.90

### 3. Presentation of the bridge set

In order to carry out analysis of the life-cycle performance for reinforced concrete structures, a set of typical RC bridges was selected. The bridges are statically determinate and have different total lengths, widths and numbers of lanes. The superstructures consist of a concrete deck with RC T-girders and crossbeams, as shown in Fig. 2. The bridge decks have a flange thickness of 10 cm and a concrete cover of 3 or 4 cm. Table 1 presents a summary of the characteristics of the superstructure, geometry and cross section in these bridges.

Based on Table 1, 18 bridges were designed to resist bending effects due to the most critical loads according to the French codes (B.A.E.L 91, Circulaire 79-25 (1979), Fascicule N° 61). The safety margin is formulated in terms of the bending moments, where  $M_R$  represents the load carrying capacity moment and  $M_a$  the total applied moment at mid-span. The bending reinforcement area was taken at the critical cross section, thus any change in the reinforcement area along the span was taken into account. Then, the corresponding safety margin (ultimate limit state) can be written as

$$Z = M_R - M_a \tag{24}$$

The ultimate bending moment  $M_R$  is calculated according to the rules provided by the French standard. Then the probability of failure  $P_f$  is accordingly estimated as

$$P_f = P(M_R - M_a \leq 0) \tag{25}$$

As specified, the FORM method is applied to determine reliability indexes. In this method, only the first order term of the Taylor series is considered and consequently, it is designated as the first order reliability method or FORM method Melchers (1999). In this paper, many variables listed in Table 2, are involved hence tangent to the limit state (Eq. (24)) is a tangent hyperplane.

Thus the reliability index  $\beta$  such as  $P_f = \Phi(-\beta)$  was used as a performance index, where  $\Phi(\cdot)$  is the probability function of the standard normal variable. Table 2 synthesises the basic variables

Table 2 Basic variables related to the safety margin

VARIABLES	DISTRIBUTION	MEAN OR BIAS	STANDARD DEVIATION OR COEFFICIENT OF VARIATION
<b>Geometric variables</b>			
Flange thickness	Deterministic	Nominal value	-
Flange width	Deterministic	Nominal value	-
Web width	Deterministic	Nominal value	-
Effective depth	Normal	Nominal value + 8 mm	3.6 mm*
Steel reinforcement	Lognormal	Nominal value	5%
Number of layers	Deterministic	Nominal value	-
Distance of steel layers	Deterministic	Nominal value	-
Steel centre of gravity	Normal	Nominal value	5%
Height of steel packet	Deterministic	Nominal value	-
<b>Material mechanical properties</b>			
Yield steel strength	Normal	Nominal value	10%
Steel deformation	Deterministic	Nominal value	-
Compressive strength of concrete	Lognormal	$f_{ck}+75$	60
<b>Loads effects</b>			
Self weight	Normal	1,00**	7%
Surface loads	Normal	1,10**	25%
Super-imposed	Normal	1,05**	10%
<b>Traffic loads effects</b>			
Traffic load $A(l)$	Deterministic	Nominal value	-
Traffic load MC120	Deterministic	Nominal value	-
$X_{LL}$	Gumbel	***	***
$DAF$	Normal	****	****

\* Standard deviation

\*\* Bias

\*\*\* Depending on loaded length and traffic flow rate

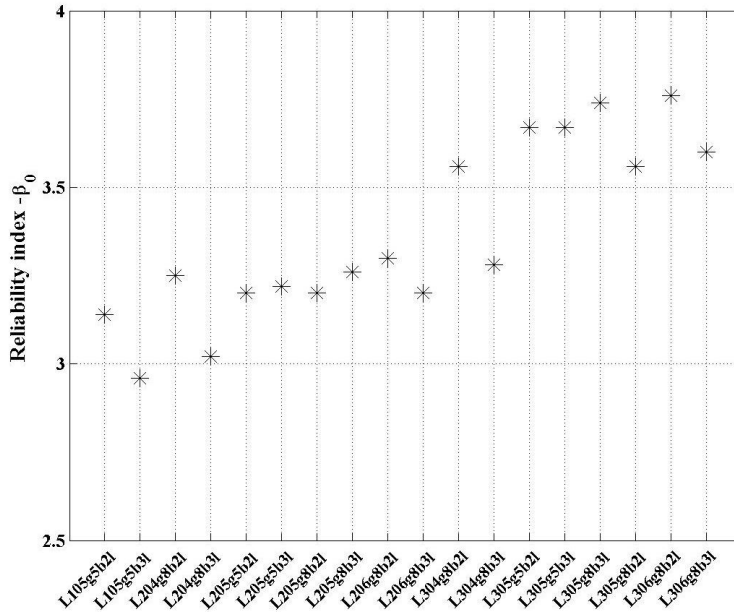
\*\*\*\* Depending on span, number of loaded lanes and pavement conditions

used for describing geometry, material and load effects. The load carrying capacity moment,  $M_R$ , on a degraded RC member is time-dependent due to the loss of reinforcement area by corrosion.

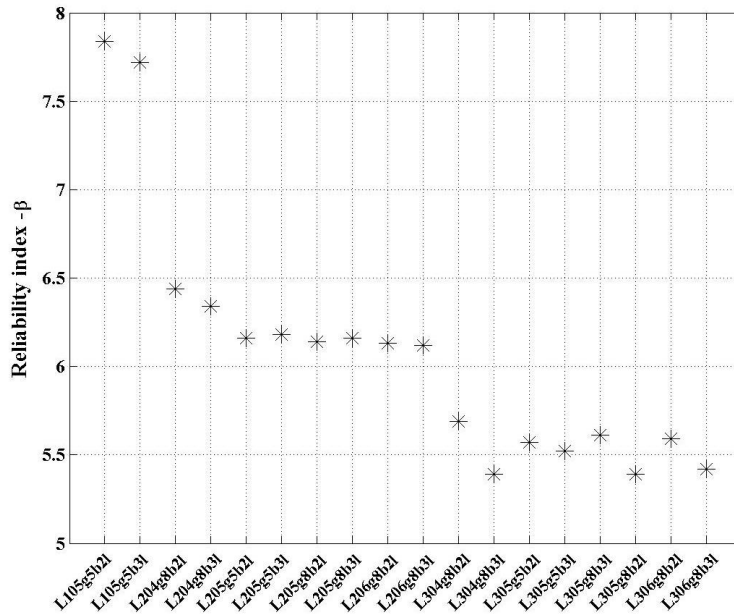
The live loads  $A(l)$  and MC120 correspond to a uniform distributed load (UDL) and a military vehicle, respectively; they are defined in the French code (Fascicule N° 61). The parameter  $X_{LL}$  is a random multiplier depending on the loaded length and traffic flow rate and  $DAF$  is the dynamic amplification factor. They have been fixed similar to the BD79 Highway Agency (2001), according to the close nature of the uniform distributed load of both models, LM1, EUROCODE 1, and  $A(l)$

$$M_{A(l)}^{prob} = M_{A(l)}^{det} \times X_{LL} \times DAF \quad (26)$$

The choice of the statistical distributions and the parameters shown in Table 2 are defined after



(a)



(b)

Fig. 3 Reliability indexes for the set of RC bridges (a)  $\beta_0$  (b)  $\beta$

a sensitivity analysis and from data available in literature, Vu Kin and Stewart (2000), Val *et al.* (1998). *T* girder cross sections are designed in a deterministic manner as required by the French standard (B.A.E.L 91) considering the most critical loading condition (in general, it is the load effect induced by MC120 vehicle). Then, a reliability analysis based on Table 2 is performed

Table 3 Statistical characteristics of the variables

<b>ENVIRONMENT</b>			
Variable	Distribution	$\mu$	CoV
Initial chloride content	Deterministic	0	-
Chloride content at concrete surface	Deterministic	Table 4	-
Critical chloride content	Deterministic	Table 4	-
Relative humidity	Deterministic	Table 4	-
Carbon dioxide content	Deterministic	0.05%	-
<b>PROPERTIES OF CONCRETE</b>			
Chloride diffusion coefficient	Deterministic	Table 4	-
Concrete porosity	Deterministic	Table 4	-
Calcium hydroxide content	Deterministic	Table 4	-
<b>GEOMETRY</b>			
Concrete cover	Normal	30-40 mm	13%
Bar diameter	Normal	32-40 mm	10%
<b>ASSESSMENT CRITERION</b>			
$w_{serv}$	Normal	0.3 mm	10%
$w_{spal}$	Normal	1.0 mm	10%
$\gamma$	Normal	Eq. (19)	
$W_{crit}$	Normal	Eq. (10)	

taking into account the design reinforcement area and the most critical bending moment (providing the  $\beta_0$  value). Another analysis is made with the same reinforcement area but with the traffic load effect from  $A(l)$  (providing the  $\beta$  value).

The  $\beta_0$  reliability index is related to the ultimate cycle identified as  $T_{\beta_0}$ . Figs. 3 (a)-(b) presents the values  $\beta$  and  $\beta_0$  for the set of RC bridges. They are identified by the length **L**, by the number of girders **g**, the number of cross beams **b**, and by the number of lanes **l**. For example, the bridge **L105g5b2l** has 10m in length, 5 girders, 5 crossbeams and 2 lanes. Fig. 3(b), the 30 m long bridges have the lowest reliability index values, whereas in the first one, they present the highest  $\beta_0$  values. This is due to the fact that, for long bridges, the  $A(l)$  load effect tends to converge with the MC120 load effect. The  $\beta_0$  reliability index is therefore the underlying reliability level of the B.A.E.L.91 code. This calculation shows that, if the MC120 vehicle is not allowed to cross these short span bridges, there is a wide range of structural strength reserve versus traffic load effects (as modeled by the French regulations), and consequently it is possible to calibrate safety factors with respect to  $\beta_0$ .

#### 4. Reliability indexes for deteriorated members

As discussed in Silva and Cremona (2004), the structural assessment of RC members can be predicted by using models described in the previous sections. In Table 3, a summary of the data used in the numerical models is presented. The rebar diameters are fixed as 32 mm and 40 mm and the concrete covers 30 mm and 40 mm values taken from the usual RC bridges designs. The factor  $\gamma$  is calculated according to a deterministic model and then modelled as a uniform variable with

Table 4 Parameter values for corrosion risk

PARAMETER	CLASS OF CORROSION RISK		
	Low	Medium	High
Critical chloride content (kg/m <sup>3</sup> )	3.0	1.4	0.6
Chloride content at concrete surface (kg/m <sup>3</sup> )	3.3; 1.54; 0.66	4.8; 2.24; 0.96	6.0; 2.80; 1.20
Chloride diffusion coefficient (10 <sup>-12</sup> m <sup>2</sup> /s)	1.0	5.0	50.0
Concrete porosity (%)	6.0	12.0	16.0
Calcium hydroxide content (%) in % of cement weight	25.0	20.0	10.0
Relative humidity (%)	80	70	65

bounds considering  $\phi=2$  and  $\phi=4$ , depending on concrete covers and rebar diameters. The critical amount of corrosion products is obtained from a Monte Carlo simulation, by assuming that steel density and rust density follow normal distributions  $N(8000\text{kg/m}^3; 800\text{kg/m}^3)$  and  $N(3600\text{kg/m}^3; 360\text{kg/m}^3)$  respectively.  $d_0$  is modelled by a lognormal distribution  $\text{LN}(12.510^{-6}\text{m}; 2.5410^{-6}\text{m})$  and concrete tensile strength is modelled using normal distribution  $N(2.54\text{ MPa}; 0.36\text{ MPa})$ .  $\alpha$ ,  $E$  and  $\nu$  are deterministic equal to 0.57; 11.5 GPa and 0.25. Some variables in Table 3 are related to durability aspects. Their statistical parameters, displayed in Table 4, have been classified into three categories depending on the corrosion risk level AFGC (2004) as dealt with in Silva and Cremona (2004).

The choice of the parameters shown in Table 4 was confirmed after a sensitivity study that shows that most of the durability variables can be chosen as deterministic. This low influence is due to the fact that some other variables (such as the yield strength of the steel) contribute more widely to the probability of failure than the durability factors in the reliability calculations Silva (2004), Silva and Cremona (2004).

## 5. Deterioration scenarios

A structural assessment for a deteriorated concrete structure is normally carried out to determine the time-dependent reliability levels. Thus, for the set of RC bridges exposed to various environment conditions (Table 5), reliability indexes are calculated. These conditions have been defined by taking combinations among the three levels of degradation parameters as defined in Table 4. There are 67 combinations of the type: MMMMM, HHHHLL, LHLLLH, LLHHHH, LHHHHL, etc. The initials L, M and H indicate Low, Medium or High classes of risk for variables in the following sequence: critical chloride content, chloride content at concrete surface, chloride diffusion coefficient, concrete porosity, calcium hydroxide content and relative humidity. For example, HHHHLL means that the critical chloride content, chloride content at concrete surface, chloride diffusion coefficient and concrete porosity, in this order, provide a High level of corrosion risk and calcium hydroxide content and relative humidity have a Low level. In Table 5, SS indicates the bridge Subset corresponding to close reliability index values, while AE means Aggressive Environment. The number that follows AE identifies the combination between critical chloride content, chloride content at concrete surface, chloride diffusion coefficient, concrete porosity, calcium hydroxide content and relative humidity.

From the 67 combinations and the analysis of the bridge set, 130 values for the corrosion

initiation (from carbonation or chloride attacks) are calculated for two concrete covers (3 and 4 cm). Then, these values can be grouped into a small number of subsets (SS1 to SS7, 3 and 4 are related to concrete cover – see Table 6), BD 79 Highway Agency (2001). In fact, Table 6 shows the mean and standard deviation related to the corrosion initiation time for each Subset given in Table 5.

Silva (2004) and Silva and Cremona (2004) show that the methodology can be extended to the following performance cycles as shown in Table 7. It presents the mean values from a probabilistic analysis based on the corrosion initiation times (issued from the reliability analysis) and material/geometrical properties (assumed as random). Nevertheless, these analyses cannot be extended to  $T_{10\%}$  and  $T_{\beta_0}$  because they depend on the bridge geometry.

## 6. Proposition of life-cycle predictions from visual inspection

Generally, the majority of damage signs in concrete structures can be detected by visual inspection. Also, this monitoring procedure can be considered as an adequate method to prevent wide evolution of the most common mechanisms of deterioration in RC structures. So, in this work, five condition assessment levels are proposed for bridges, based on visual inspection: **Level 0** - good condition; **Level 1** perceptible corrosion spots, humid zones and small cracks (0.05mm, corrosion initiation and cracking are reached); **Level 2** - cracks approximately 0.3mm wide; **Level 3**: large cracks and spalling; **Level 4**: degraded condition - 10% of the bottom layer is lost, reinforcement is exposed.

Table 5 Subsets of bridges based on the corrosion initiation time predictions

SUBSET	ENVIRONMENT	$T_i(cp=30mm)$ (year)	SUBSET	ENVIRONMENT	$T_i(cp=40mm)$ (year)
	AE2_HLHHLH	0.63		AE2_HLHHLH	1.12
	AE7_LHHHHL	0.63		AE7_LHHHHL	1.12
	AE22_LHHHLH	0.63		AE22_LHHHLH	1.12
	AE26_HHHHHH	0.63		AE26_HHHHHH	1.12
	AE36_MHHMLM	0.63		AE36_MHHMLM	1.12
	AE40_MHHMHM	0.63		AE40_MHHMHM	1.12
<b>SS1-3</b>	AE13_MMHMMM	1.19	<b>SS1-4</b>	AE13_MMHMMM	2.12
	AE41_MMHHML	1.19		AE41_MMHHML	2.12
	AE42_MMHHMH	1.19		AE42_MMHHMH	2.12
	AE58_LMHMML	1.19		AE58_LMHMML	2.12
	AE59_HMHMML	1.19		AE59_HMHMML	2.12
	AE62_LMHMMH	1.19		AE62_LMHMMH	2.12
	AE63_HMHMMH	1.19		AE63_HMHMMH	2.12
	AE11_MHMMMM	6.27		AE11_MHMMMM	11.15
	AE27_LHMLMM	6.27		AE27_LHMLMM	11.15
	AE28_HHMLMM	6.27		AE28_HHMLMM	11.15
<b>SS2-3</b>	AE31_LHMHMM	6.27	<b>SS2-4</b>	AE31_LHMHMM	11.15
	AE32_HHMHMM	6.27		AE32_HHMHMM	11.15
	AE51_MHMMLL	6.27		AE51_MHMMLL	11.15
	AE53_MHMMHL	6.27		AE53_MHMMHL	11.15

Table 5 Continued

	AE55_MHMMLH	6.27		AE55_MHMMLH	11.15
	AE57_MHMMHH	6.27		AE57_MHMMHH	11.15
	AE6_LLHHHH	6.72		AE6_LLHHHH	11.95
	AE49_LMMHHM	9.44		AE49_LMMHHM	16.78
	AE50_HMMHHM	9.44		AE50_HMMHHM	16.78
	AE56_MLMMHH	11.28		AE56_MLMMHH	20.05
	AE8_LMMMMM	11.92		AE8_LMMMMM	21.19
	AE9_HMMMMM	11.92		AE9_HMMMMM	21.19
	AE17_MMMMMM	11.95		AE1_MMMMMM	21.24
	AE1_MMMMMM	11.95		AE14_MMMLMM	21.24
	AE14_MMMLMM	11.95		AE15_MMMHMM	21.24
	AE15_MMMHMM	11.95		AE16_MMMMLM	21.24
	AE16_MMMMLM	11.95		AE17_MMMMHH	21.24
	AE18_MMMMML	11.95		AE18_MMMMML	21.24
	AE19_MMMMML	11.95		AE19_MMMMML	21.24
<b>SS3-3</b>	AE43_LMMLLM	11.95	<b>SS3-4</b>	AE43_LMMLLM	21.24
	AE44_HMMLLM	11.95		AE44_HMMLLM	21.24
	AE45_LMMHLM	11.95		AE45_LMMHLM	21.24
	AE46_HMMHLM	11.95		AE46_HMMHLM	21.24
	AE47_LMMLHM	11.95		AE47_LMMLHM	21.24
	AE48_HMMLHM	11.95		AE48_HMMLHM	21.24
	AE37_MLLMHM	15.83		AE37_MLLMHM	28.14
	AE38_MHLMHM	15.83		AE38_MHLMHM	28.14
	AE39_MLHMHM	15.83		AE39_MLHMHM	28.14
	AE21_LLHHLH	16.81		AE21_LLHHLH	29.88
	AE3_HLHHLH	16.81		AE3_HLHHLH	29.88
	AE29_LLMHMM	18.87		AE29_LLMHMM	33.55
	AE30_HLMHMM	18.87		AE30_HLMHMM	33.55
<b>SS4-3</b>	AE25_HLHHHL	21.91	<b>SS5-4</b>	AE25_HLHHHL	38.95
	AE35_MLHMLM	21.91		AE35_MLHMLM	38.95
	AE60_LMLMMH	22.55		AE60_LMLMMH	40.10
	AE61_HMLMMH	22.55		AE61_HMLMMH	40.10
	AE54_MLMMLH	28.19		AE54_MLMMLH	50.12
	AE4_HHLLHH	31.37		AE4_HHLLHH	55.77
	AE5_LHLLLH	31.37		AE5_LHLLLH	55.77
<b>SS5-3</b>	AE20_HHLLLL	31.37	<b>SS6-4</b>	AE20_HHLLLL	55.77
	AE24_LHLLHL	31.37		AE24_LHLLHL	55.77
	AE34_MHLMML	31.37		AE34_MHLMML	55.77
	AE10_MLMMMM	31.66		AE10_MLMMMM	56.29
	AE12_MMLMMM	31.66		AE12_MMLMMM	56.29
	AE52_MLMMHL	38.63		AE52_MLMMHL	68.67
<b>SS6-3</b>	AE23_LLLLHH	39.16		AE23_LLLLHH	69.63
	AE33_MLLMLM	39.58		AE33_MLLMLM	70.36
	AE64_MMLLML	59.73	<b>SS7-4</b>	-	-
<b>SS7-3</b>	AE65_MMLLMH	59.73		-	-
	AE66_LMLMML	59.73		-	-
	AE67_HMLMML	59.73		-	-

Table 6 Average and standard deviation values

SUBSET	MEAN (YEARS)	STANDARD DEVIATION (YEARS)	SUBSET	MEAN (YEARS)	STANDARD DEVIATION (YEARS)
SS1-3	0.93	0.29	SS1-4	1.66	0.52
SS2-3	6.84	1.22	SS2-4	12.16	2.17
SS3-3	12.93	1.91	SS3-4	21.16	0.30
SS4-3	21.11	1.76	SS4-4	30.18	2.43
SS5-3	31.05	1.16	SS5-4	39.53	0.66
SS6-3	39.12	0.48	SS6-4	55.19	2.06
SS7-3	59.73	0.00	SS7-4	69.55	0.85

Table 7 Average values of the performance cycles for 30 and 40 mm cover ( $i_{corr}=2.5\mu\text{A}/\text{cm}^2$ )

SUBSET	$T_i$ (yrs)	DIAMETER OF THE BAR ( $\phi$ 40mm)			SUBSET	$T_i$ (yrs)	DIAMETER OF THE BAR ( $\phi$ 40mm)		
		$T_{crack}$ (yrs)	$T_{serv}$ (yrs)	$T_{spal}$ (yrs)			$T_{crack}$ (yrs)	$T_{serv}$ (yrs)	$T_{spal}$ (yrs)
		SS1-3	0.93	2.54			3.42	5.46	SS1-4
SS2-3	6.84	8.45	9.33	11.37	SS2-4	12.16	13.93	15.04	17.65
SS3-3	12.93	14.54	15.42	17.46	SS3-4	21.16	22.93	24.04	26.65
SS4-3	21.11	22.72	23.60	25.64	SS4-4	30.18	31.95	33.06	35.67
SS5-3	31.05	32.66	33.54	35.58	SS5-4	39.53	41.30	42.41	45.02
SS6-3	39.12	40.73	41.61	43.65	SS6-4	55.19	56.96	58.07	60.68
SS7-3	59.73	61.34	62.22	64.26	SS7-4	69.55	71.32	72.43	75.04

Adapted from Silva (2004), Silva and Cremona (2004a)

Table 7 (Silva 2004, Silva and Cremona 2004) represents a first approximation for main time degradation prediction by Subsets as explained in section 5. It constitutes an example of very easy-to-use information for rough performance cycle prediction.

In the following paragraphs this assessing serviceability cycles method will be coupled with a set of partial safety factors more suitable to the real degradation state of the structural element (girders) caused by corrosion phenomena.

## 7. Deriving partial safety factors suitable to existing structures

### 7.1 Existing assessment rules

Assessment can be defined as a set of activities used to determine the safe load capacity of an existing structure. Load capacity evaluation can be carried out using a wide range of approaches depending on the level of information available and accuracy required. Generally, a structure evaluation involves comparing the actual capacity with the capacity required to resist the specified loading. Applied methods can be based on simple deterministic approaches, semi-probabilistic methods through sophisticated reliability techniques.

In the probabilistic approach, the stress  $S$  and strength  $R$  of a structural element are randomly described because their values are not perfectly known. In reliability assessment, if the criterion

related to the limit state results in  $R < S$  then limit state is exceeded. The probability  $p_f$  of the event  $R < S$  characterizes the reliability level of the component with regard to the considered limit state  $p_f = P(R < S)$ , where  $p_f$  is the *probability of failure*.

The semi-probabilistic approach of structural safety is used in many design codes. It consists of general rules that provide safety for a structural element and it also considers both the characteristic values of the relevant design parameters and the partial safety factors. It replaces the probability calculation by verifying a criterion involving characteristic values of  $R$  and  $S$ , denoted  $R_k$  and  $S_k$ , and partial factors  $\gamma_R$  and  $\gamma_S$  which may be represented as shown in Eq. (27). The so-called partial safety format is said to be semi-probabilistic, because it takes into account the application of statistics and probability in the evaluation of the input data, formulation of assessment criteria and determination of load and resistance factors. Actually, this approach applies partial safety factors to all important design parameters, e.g., different factors for dead and live loads, different strengths, for instance, in the resistance of RC beams.

In addition, these partial safety factors must cover a great number of uncertainties induced by parameters omitted during the assessment. Also, they are fixed to provide designs not too different from designs carried out following former design methods. In fact, their essential function is to cover the variability in structural behavior and loading Calgaro (1996). Actually, the standards aim to provide a minimum acceptable performance related to a *failure probability* called  $\rho_f^{\text{target}}$ ; so, the structural assessment is aimed at verifying  $\rho_f \leq \rho_f^{\text{target}}$  or, in others words,  $\beta \geq \beta_{\text{target}}$ . Thus, the partial safety factors can be defined as the ratio between the characteristic values and the design values as follows

$$\gamma_R = \frac{R_k}{R_d}; \left( \phi = \frac{R_d}{R_k} \right) \text{ and } \gamma_S = \frac{S_d}{S_k} \quad (27)$$

## 7.2 Some restrictions for using design rules for assessment

It is important to notice that the rules presented in design codes constitute a set of prescribed regulations that are only valid in a certain context. Thus, in order to be applicable to a bridge they must conform to the design code in the following features: type of bridges; the methods used in the structural analysis; the actual traffic loading on the bridge and so on. In existing structures, particular structural situations often exist. Sometimes, the application of design codes in reliability assessment becomes inappropriate on account of the presence of nonconforming details in existing structures. Design codes present safety margins which, in general, exceed those that are reasonably acceptable for assessing existing bridges. This is due to the lack of knowledge regarding damage scenarios and actual traffic conditions in existing structures. Both traffic and damage can be evaluated and then furnish more reliable data about old bridges. This way, partial safety factors can be reduced while maintaining the same level of structural reliability. Information about the structures can be increased with further investigations and this can justify further reductions (or augmentation) in partial safety factors.

In this paper, the proposed calibration method for partial safety factors is based on visual inspection results (section 6 - Silva and Cremona (2004)). Actually, safety factors are adjusted taking into account the damage condition of the assessed element. Consequently, this method gives a more realistic and rational set of partial safety factors, because damage characteristics are considered. It means that the actual load capacity is adapted to the damage state. In addition, the security level  $\beta$  ensured that the existing structures approach the minimum acceptable performance

value  $\beta_0$  (implicit in the standards). In fact, as it has been said, the safety factors consider the variability in structural behavior and loading. However, the required safety margin is reduced with age due to degradation phenomena, increase in traffic. Finally, the optimum safety level in a new design is greater than in an existing structural element, so the necessity of establishing more suitable safety factors is clear.

### 7.3 Proposed calibration method

The calibration of safety factors is based on the minimum acceptable performance level  $\beta_0$  and not on the target performance level,  $\beta_{\text{target}}$ , commonly utilized. In fact the target reliability index has an average reliability sense, i.e., it represents a typical performance level for all the structure. For this reason, its use in the calibration method is not advisable; since  $\beta_0$  considers structural low reliability elements (low load capacity) match structural high safety elements.

The performance index,  $\beta_0$ , represents a particular safety level for each structural element (a girder, for example). In this paper, it indicates a proper safety level (Eq. (24)) for the most critical cross section of each examined bridge. In this way, these structural elements must have reliability indexes higher than  $\beta_0$  ( $\beta > \beta_0$ ), or in other words, these elements present a safety structural reserve (Fig. 3) which makes it possible to adjust the partial safety factors.

The first step to begin the calibration procedure is to calculate the  $\beta_0$  (section 3) of the critical cross section. Then, a preliminary set of partial safety factors is established. To recalculate this set of factors, the safety factors applied to material strength, concrete ( $\gamma_c$ ) and steel ( $\gamma_s$ ), are considered. In the solicitation side, two other safety factors are identified. The first,  $\gamma_{DL}$ , applied to the dead load ( $DL$ ) and the second,  $\gamma_Q$ , to the most severe loading condition ( $Q$ ), in this case MC120 (section 3). The limit state function, defined by a straight line ( $R=S$ ) as a function of the partial safety factors, is expressed by

$$(\gamma_c, \gamma_s)R = \gamma_{DL} DL + \gamma_Q Q \quad (28)$$

In order to have a limit state as a function of three independent variables, the safety factor  $\gamma_{DL}$  is fixed. Thus, if the three independent variables are known, the partial safety factors in Eq. (28) can be defined from  $\gamma_{DL}$ . So, for a given  $\gamma_{DL}$ , the parameters  $\gamma_c$ ,  $\gamma_s$  and  $\gamma_Q$  are obtained. As a result, the initial set of safety factors is  $(1/\gamma_{DL} \gamma_c; 1/\gamma_{DL} \gamma_s; \gamma_Q/\gamma_{DL})$  and the adopted values are:  $\gamma_c = 1.5$ ;  $\gamma_s = 1.15$ ;  $\gamma_Q = 1.35$  and  $\gamma_{DL} = 1.35$ . Then, Eq. (28) can be expressed as

$$DL = \left( \frac{1}{\gamma_{DL} \gamma_c}, \frac{1}{\gamma_{DL} \gamma_s} \right) R - \left( \frac{\gamma_Q}{\gamma_{DL}} \right) Q \quad (29)$$

Thus, the determination of  $\beta_0$  (section 3); the choice of an initial set of safety factors as discussed and the safety margin definition (Eq. (24)) used in the reliability analysis ( $\beta$ ) denote the end of the first stage of the calibration process.

The second stage of the method aims to determine a set of safety factors which fulfills the condition  $\beta \approx \beta_0$ . To reach this goal, Eq. (29) is completely developed, considering the variable  $R$  replaced by the *load carrying capacity moment* ( $M_R$ ) (calculated according to the rules provided by the French standard), the dead load ( $DL$ ) and MC120 ( $Q$ ) replaced by the bending moments,  $M_{DL}$  and  $M_Q$ , respectively. The  $M_R$  moment is determined according to the following expression

$$M_R = A_s f_s z \quad (30)$$

where

$$z = d - 0.4 d \alpha_u \quad (30a)$$

$$\alpha_u = 1.25 \left( 1 - \sqrt{1 - 2 \left( \frac{\gamma_{DL} M_{DL} + \gamma_Q M_Q}{b d^2 f_c} \right)} \right) \quad (30b)$$

where  $A_s$  represents the steel reinforcement;  $f_s$  yield strength of steel;  $z$  the distance between the compression and tension resultants in the cross beam section;  $d$  effective depth;  $f_c$  compressive strength of concrete and  $b$  flange width, Silva (2004).

The load effects due to dead load are composed of three bending moments (Table 2),  $M_{SL}$ ,  $M_{SI}$  and  $M_{SW}$ . So, Eq. (29) can be written as Silva 2004

$$\left( \frac{\gamma_{DL}}{\gamma_{DL}} \right) (M_{SL}, M_{SI}, M_{SW}) = \left( \frac{1}{\gamma_{DL} \gamma_c}, \frac{1}{\gamma_{DL} \gamma_s} \right) M_R - \left( \frac{\gamma_Q}{\gamma_{DL}} \right) M_Q \quad (31)$$

$$M_{SW} = \left( \frac{1}{\gamma_{DL} \gamma_c}, \frac{1}{\gamma_{DL} \gamma_s} \right) M_R - \left( \frac{\gamma_{DL}}{\gamma_{DL}} \right) (M_{SL}, M_{SI}) - \left( \frac{\gamma_Q}{\gamma_{DL}} \right) M_Q \quad (31a)$$

where  $M_{SL}$  is the *surface load* bending moment,  $M_{SI}$  the *super-imposed* bending moment that accounts for non-structural elements permanently fixed to the bridge such as road signs, ducts, rails or parapets and  $M_{SW}$  self weight of the structural member. In Eq. (31a), all variables are deterministic, i.e., their values are equal to the mean.

Eq. (31a), when developed, can be expressed as

$$\frac{R_1 A_s f_e d}{2} \left( 1 + \sqrt{1 - \left( \frac{2(M_{SW} + M_{SL} + M_{SI}) + 2R_3 M_Q}{R_2 b d^2 f_c} \right)} \right) - (M_{SW} + M_{SL} + M_{SI}) - R_3 M_Q = 0 \quad (32)$$

where  $R_1=1/\gamma_s \gamma_{DL}$ ;  $R_2=1/\gamma_c \gamma_{DL}$  and  $R_3= \gamma_Q/\gamma_{DL}$ . Also, this expression carries out to a second degree equation ( $(1/a_1^2)M_{SW}^2 + (2a_3/a_1 + a_2)M_{SW} + (a_3^2 - a_4) = 0$ ), where the self weight bending moment values are the roots. The equation coefficients' are in function of the material properties, geometry and bending moments, then:  $a_1(R_1, A_s, f_s, d)$ ;  $a_2(R_2, b, d, f_c)$ ;  $a_3(R_3, M_{SL}, M_{SI}, M_Q, a_1)$  and  $a_4(M_{SL}, M_{SI}, M_Q, a_2)$ .

An optimization routine gives a  $M_{SW}$  value in each iteration, then the maximum root is integrated in the function limit state (Eq. (24)) modeled by a normal distribution (bias=1.0; coefficient of variation=7%). As a result, a reliability index is given ( $\beta$ ). Thus  $\beta$  is compared with  $\beta_0$  and if the result differences of the minimization function ( $\beta-\beta_0$ ) keep a tolerance of  $10^{-4}$ , the set of safety factors is considered suitable.

In this paper, this methodology is applied to all performance cycles:  $T_i$ ,  $T_{crack}$ ,  $T_{serv}$ ,  $T_{spal}$  and  $T_{10\%}$ .

#### 7.4 Calibration method application

In this section, the calibration methodology is applied to one bridge which is noted L205g5b31

Table 8 Partial safety factor reduction set of the L205g5b3l bridge (concrete cover 4cm)

Subset	$T_i$ (%)			$T_{crack}$ (%)			$T_{serv}$ (%)			$T_{spat}$ (%)			$T_{10\%}$		
	$\gamma_c$	$\gamma_s$	$\gamma_Q$	$\gamma_c$	$\gamma_s$	$\gamma_Q$	$\gamma_c$	$\gamma_s$	$\gamma_Q$	$\gamma_c$	$\gamma_s$	$\gamma_Q$	$\gamma_c$	$\gamma_s$	$\gamma_Q$
SS1-4	-6.8	-20.4	-46.8	-8.0	-19.8	-46.3	-7.4	-20.1	-46.7	-7.6	-20.0	-46.7	-8.0	-19.8	-46.3
SS2-4	-6.7	-20.4	-46.7	-8.0	-19.8	-46.3	-7.5	-20.1	-46.7	-6.7	-19.8	-47.1	-8.0	-19.8	-46.3
SS3-4	-7.1	-20.2	-46.9	-8.1	-19.8	-46.1	-7.3	-20.1	-46.7	-7.6	-20.0	-46.6	-8.1	-19.8	-46.1
SS4-4	-6.9	-20.3	-46.8	-8.0	-19.7	-46.2	-7.6	-20.0	-46.6	-7.8	-19.9	-46.5	-8.0	-19.7	-46.2
SS5-4	-7.2	-20.2	-46.6	-7.5	-20.0	-45.1	-7.8	-19.9	-46.5	-7.9	-19.8	-46.3	-7.5	-20.0	-45.1
SS6-4	-7.9	-19.7	-45.5	-6.9	-19.9	-42.8	-8.2	-19.5	-45.1	-8.1	-19.4	-45.0	-6.9	-19.9	-42.8
SS7-4	-7.5	-19.9	-45.3	-6.6	-20.2	-43.0	-6.6	-20.4	-43.6	-6.6	-20.3	-43.6	-6.6	-20.2	-43.0
$\mu$	-7.2	-20.1	-46.4	-7.6	-19.9	-45.1	-7.5	-20.0	-46.0	-7.5	-19.9	-46.0	-7.6	-19.9	-45.1
$\sigma$	0.41	0.27	0.67	0.61	0.18	1.56	0.50	0.27	1.19	0.57	0.28	1.24	0.61	0.18	1.56

Table 9 Single set of safety factors for L205g5b3l bridge

	L205g5b3l														
	$T_i$ (%)			$T_{crack}$ (%)			$T_{serv}$ (%)			$T_{spat}$ (%)			$T_{10\%}$		
	$\gamma_c^1$	$\gamma_s^1$	$\gamma_Q^1$	$\gamma_c^1$	$\gamma_s^1$	$\gamma_Q^1$	$\gamma_c^1$	$\gamma_s^1$	$\gamma_Q^1$	$\gamma_c^1$	$\gamma_s^1$	$\gamma_Q^1$	$\gamma_c^1$	$\gamma_s^1$	$\gamma_Q^1$
$\mu$	1.39	0.92	0.72	1.38	0.92	0.72	1.39	0.92	0.72	1.38	0.92	0.73	1.40	0.93	0.82
$\sigma$	0.01	0	0.01	0.01	0	0.01	0.01	0	0.02	0.01	0	0.02	0.01	0.01	0.03

(section 3). The critical cross section has a concrete cover of 4cm and a bar diameter of 40mm. The bridge is subjected to the environmental conditions shown in Table 5 and the performance cycles grouped into a subset are those in Table 7. Table 8 presents the reduction set to be applied to safety factors for each performance cycle. In this case, the minimum acceptable performance level is 3.22 and the initial set of safety factors is  $(1/1.5\gamma_{DL}, 1/1.5\gamma_{DL}, 1.35/\gamma_{DL})$  (section 7.3), where  $\gamma_{DL}$  is equal to 1.35 (Silva 2004). These safety factors are independent. The minus sign, shown in Table 8, indicates a reduction in the original value of the partial safety factors (section 7.3).

Suggested reduction percentages for safety factors of a given bridge, are grouped into subsets following the same procedure applied to the performance cycles. For example, in the hatch cells, Table 8, the new set of factors is roughly  $\gamma_c^1 = 1.40[(1-0.068)1.5]$ ;  $\gamma_s^1 = 0.92$ ,  $\gamma_{DL} = 1.35$  and  $\gamma_Q^1 = 0.72$ . The reduction in the three safety factors is not surprising. In fact, the  $A(t)$  traffic provides the reliability indexes,  $\beta$ , higher than  $\beta_0$ . So, it is intuitive to think that the safety factors can be reduced taking into account this *safety reserve*. This is owing to the unchanged design values (MC120 load and the characteristic material values). It may be noticed that the calibration method gives low scattering values of reduction percentages (see  $\sigma$  values - Table 8), among the bridge subsets, as well as in a given subset. As a result, it seems reasonable to propose a single set of reduction safety factors for the given bridge (Table 9).

## 8. Conclusions

It is possible to calibrate partial safety factors even when a damaged structural element still presents a safety level higher than the index  $\beta_0$  (allowable threshold). A set of safety factors which

are more adapted to the principal stages of performance cycles is obtained. Values of reduction percentages among the bridge subsets undergoes negligible scattering. From this fact it is possible to propose a single set of reduction safety factors for a given bridge.

In the proposed calibration method,  $M_{SW}$  is the maximum root in Eq. (32) and it can be considered as a link between the safety margin (ultimate limit state), Eq. (24), and Eq. (32). Actually, when this root is integrated in the limit state function (Eq. (24)), it intrinsically represents the value of the self weight associated with the critical load condition (MC120). Once  $M_{SW}$  is integrated in the safety margin,  $\beta$  index is determined considering the  $A(l)$  traffic load. This way,  $\beta$  approaches  $\beta_0$  and the safety reserve between the two indexes is transformed into a set of safety factors adjusted to  $\beta_0$ .

According to Silva (2004), the influence of structural characteristics is verified by comparing three bridges with different structural configurations. Nevertheless, a slight influence of structural features on the calibration sets may be observed. Such a result allows considering a single set of safety factors independently from the bridge structural characteristics.

## Acknowledgements

The authors would like to acknowledge and thank the financial support provided by the Laboratoire National des Ponts et Chaussées (LNPC) in Paris and the University of Brasilia (UnB). Special thanks to Dr. Christian Cremona for the continuing support as thesis advisor and for encouraging my research.

## References

- AFGC (2004), *Conception des Bétons pour une Durée de Vie Donnée des Ouvrages – Maîtrise de la Durabilité vis-à-vis de la Corrosion des Armatures et de l'Alcali-Réaction*, Association Française de Génie Civil. (in French)
- Andrade, C., Alonso, C. and Molina, F.J. (1993), "Cover cracking as a function of bar corrosion: Part 1 - experimental test", *Mater. Struct.*, **26**(162), 453-464.
- B.A.E.L 91 modifiées 99 (2000), *Règles Techniques de Conception et de Calcul des Ouvrages et Constructions en Béton Armé suivant la Méthode des États-Limites*, Eyrolles. (in French)
- BD 79 Highway Agency (2001), *Level 4 and Level 5 Methods of Assessment for Bridges*.
- Calgaro, J.A. (1996), *Introduction aux Eurocodes – Sécurité des Constructions et Bases de la Théorie de la Fiabilité*, Presses de l'école nationale des ponts et chaussées. (in French).
- Catbas, F.N., Susoy, M. and Frangopol, D.M. (2008), "Structural healthy monitoring and reliability estimation: Long span truss bridge application with environmental monitoring data", *Eng. Struct.*, **30**(9), 2347-2359.
- Circulaire N° 79-25, (1979), *Instruction Technique sur les Directives Communes de 1979 relatives au Calcul des Constructions (D.D.79)*, Marchés Publics, Décision n.6-79 du groupe permanent d'étude des marches de travaux. (in French)
- Cui, H., Wang, H. and Zhang, L. (2011), "Safety management of reinforced concrete bridges in china and evaluation methods for strength of existint RC bridges with crack", *Proceedings of International Conference on Multimedia Technology (ICMT)*, Hangshou, China.
- Czarnecki, A.A. and Nowak, A.S. (2008), "Time-variant reliability profiles for steel girder bridges", *Struct. Safety*, **30**, 49-64.
- EUROCODE 1 - ENV 1991-1 (1996), *Norme Européenne : Eucorode 1: Bases de calculs et Actions sur les*

- Structures - Partie I: bases de calcul*, AFNOR. (in French)  
Fascicule N° 61, *Conception, Calcul et Épreuves des Ouvrages d'art, Titre II - Programmes de Charges et Épreuves des Ponts-Routes*, Cahier des Prescriptions Communes Applicables aux Marchés de Travaux Publics relevant des Services de l'équipement (in French).
- Ishida, T. and Maekawa, K. (2000), "Modelling of pH profile in pore water based on mass transport and chemical equilibrium theory", *Translation from proceedings of Japan Society of Civil Engineering*, May.
- Liu, Y. and Weyers, R.E. (1998), "Modelling the time-to-cracking in chloride contaminated reinforced concrete structure", *ACI Mater. J.*, **95**(6), 675-681.
- Melchers, R.E. (1999), *Structural Reliability Analysis and Prediction*, Wiley, UK.
- Papadakis, V.G., Vayenas, C.G. and Fardis, M.N. (1991a), "Experimental investigation and mathematical modelling of the concrete carbonation problem", *Chem. Eng. Sci.*, **46**(5/6) 1333-1338.
- Papadakis, V.G., Vayenas, C.G. and Fardis M.N. (1991b), "Fundamental modelling and experimental investigation of concrete carbonation", *ACI Mater. J.*, **88**(4), 363-373.
- Petryna, Y.S. and Kratzig, W.B. (2005), "Compliance-based structural damage measure and its sensitivity to uncertainties", *Comput. Struct.*, **83**(4), 1113-1133.
- Sharifi, Y. and Paik, J.K. (2010), "Ultimate strength reliability analysis of corroded steel-box girder", *Thin Wall. Struct.*, **49**, 157-166.
- Silva, R. (2004), *Contribution à l'Analyse Probabiliste de la Performance des Ponts en Béton Armé, Ouvrages d'art OA50*, Laboratoire Central des Ponts et Chaussées. (in French)
- Silva, R. and Cremona, C. (2004a), "Some considerations on the performance cycle analysis of concrete girders in France", *Struct. Infrastruct. Eng.*, **1**(3), 207-220.
- Thoft-Christensen, P. (2000), "Modelling of deterioration of reinforced concrete structures", *Reliability and optimization of structures systems, Proceedings of the ninths IFIP WG 7.5 working conference on reliability and optimization of structural systems*, Munich, Germany.
- Thomos, G.C. and Trezos, C.G. (2011), "Reliability based calibration of the capacity design rule of reinforced concrete beam-column joints", *Comput. Concrete*, **8**(6), 631-645.
- Val, D.V., Stewart, M.G. and Melchers, R.E. (1998), "Effect of reinforcement corrosion on reliability of highway bridges", *Eng. Struct.*, **20**(11), 1010-1019.
- Vu Kim, A.T. and Stewart, M.G. (2000), "Structural reliability of concrete bridges including improved chloride-induced corrosion models", *Struct. Saf.*, **22**(3), 313-333.
- Xiangyang, W. and Pei, Z. (2010), "Reliability analysis and life prediction of beam bridge base on more failure method", *Proceedings of Ninth International Symposium on Distributed Computing and Applications to Business, Engineering and Science*, Hong Kong, August.